VISCOELASTIC REPRESENTATION OF SUCKER ROD PUMP SYSTEMS

Sheldon Wang, Midwestern State University
Lynn Rowlan and Carrie Anne Taylor, Echometer Company
Abbey Henderson, Sean T. Aleman, and Trent Creacy
Midwestern State University- Undergraduate Students

ABSTRACT

The issues of leakage with respect to the clearance between the pump plunger outer surface and the pump barrel inner surface and other operation conditions have been revisited in this paper using viscoelastic models. Both Poiseuille flow rate due to the pressure difference and Couette flow rate due to the plunger motion have been considered. The purpose of this study is to explore the possibility of representing the entire downhole pump system with a simple viscoelastic model. We have explored both Kelvin and Maxwell viscoelastic models along with their counterparts in electrical circuits simulated with NI Multisim. By using the time-dependent bridle force measured with the dynamometer as the input to the viscoelastic models, we have obtained the displacement responses simulated with Mathworks Matlab programs which match closely with the actual experimental measurements. Experimental validations have been planned and partially implemented in the McCoy School of Engineering at Midwestern State University.

INTRODUCTION

Throughout a typical petroleum reservoir's productive life, natural lift force due to fluid pressure tends to decay and to diminish. Therefore, artificial lift methods are commonly utilized to transfer the oil and gas from the formation to the surface. The most popular artificial lift means are sucker rod pumping system, hydraulic pumping system, electric submersible pumping system, and gas lift system [3]. As one of the earliest inventions for oil fields in land, sucker rod pumping system proves to be one of the most efficient and popular artificial lift systems in the Petroleum Industry [1]. In this paper, we focus more on the production efficiency with respect to the pump mechanisms, which consists of a moving contact area between the traveling unit (plunger), a chamber with a so-called traveling valve, and the tube or barrel with a so-called standing valve [4]. It is very often that a clearance between 3 to 8 mills (one thousandth of an inch) is recommended to avoid the direct contact (abrasion) between the plunger and the tube and to allow the unimpeded passage of sands and particles within the oil mixture [5]. In practice, it has been reported that the leakage is related to the clearance, or two times the gap size, defined as the difference between the inner diameter of the barrel and the outer diameter of the plunger [1]. In the existing literature, it has been established that for viscous fluid to squeeze through a narrow annulus channel, the required pressure gradient or pressure drop given a fixed channel length will be proportional to the clearance to the power of three [2] [6]. In this paper, we would like to introduce viscoelastic models to mimic sucker rod pump unit behavior in particular the piston like motion between the plunger and the barrel.

THEORY AND MODELING

We introduce first the Kelvin based viscoelastic model in a dynamic case as shown in Fig. 1, essentially a typical Kelvin viscoelastic setup for creep test combined in series with a spring with a stiffness k and a mass m. The displacement of the parallel section of the stiffness k_o and the dashpot c_o shares the same displacement $u_2(t)$, whereas the displacement of the stiffness k is denoted as $u_1(t)$. Since the mass m is connected with the stiffness k in series, the total displacement of the mass u(t), is a combination of the two displacements $u_1(t)$ and $u_2(t)$. In general, the external load F(t) is applied to the mass m. Notice here this external load will be replaced with the bridle force measured by the dynamometer when we replace the entire downhole suck rod pump system with the Kelvin viscoelastic model. We can imagine that in creep test, we can simply add a dead weight W_o in addition to the weight mg of the mass m.

Using the procedure to identify dynamic and kinematic governing equations, consider for each section in series we have consequent continuity of axial forces and combination of displacements and for each section in parallel we have consequent continuity of displacements and combination of forces, we have

$$ku_1(t) = k_o u_2 + c_o \dot{u}_2$$
$$ku_1(t) = F(t) - m\ddot{u}$$

Using the kinematic relationship u(t)=$u_1(t) + u_2(t)$, we obtain the following third-order governing equation for u_2(t),

$$\frac{mc_o}{k}\dddot{u}_2 + \frac{m}{k}(k + k_o)\ddot{u}_2 + c_o\dot{u}_2 + k_o u_2 = F(t)$$

Let's look at two special cases. First of all, with no dashpot, namely, c_o=0. In this case, we have

$$k_o u_2 = ku_1$$

hence

$$u=u_1 + u_2 = \frac{k+k_o}{k}u_2$$

Finally, the governing dynamic equation yields the familiar spring-mass vibration system for this setup with two stiffness or springs connected in series

$$m\ddot{u} + \frac{kk_o}{k+k_o}u = F(t)$$

with the familiar effective stiffness of two springs in series.

The second special case corresponds to the infinite stiffness k, namely, k→ ∞, consequently, we have $u_1 \to 0$ and $u(t) = u_2(t)$. Finally, we recover the familiar spring-mass-dashpot vibration system

$$m\ddot{u} + c_o\dot{u} + k_o u = F(t).$$

To facilitate the solution, we can rewrite the third-order viscoelastic vibration system with a standard dynamical system format,

$$\dot{\mathbf{y}} = \mathbf{A}\mathbf{y} + \mathbf{f},$$

with the state variable $\mathbf{y} = < u_2, \dot{u}_2, \ddot{u}_2 >$, and

$$\boldsymbol{A} = \begin{bmatrix} 0 & 1 & 0 \\ 0 & 0 & 1 \\ -\frac{kk_o}{mc_o} & -\frac{k}{m} & -\frac{k+k_o}{c_o} \end{bmatrix} \text{ and } \mathbf{f}=\begin{bmatrix} 0 \\ 0 \\ \frac{kF}{mc_o} \end{bmatrix}$$

Let's consider the Maxwell based viscoelastic model in a dynamic case as shown in Fig. 1, essentially a typical Maxwell viscoelastic setup for relaxation test combined a mass m in series connecting with two parallel branches, one with a stiffness k and another one with a stiffness k_o and a dashpot c_o in series. The displacement of the parallel section shares the same value u(t), whereas the displacement of the stiffness is denoted as u_2(t) and the dashpot c_o connected in series with the stiffness k_o as u_1(t). Since the displacement of the stiffness k is u(t), naturally, the total displacement of the mass u(t) is a combination of the two displacements u_1(t) and u_2(t) within one of the parallel branches. In general, the external load F(t) is applied to the mass m. Likewise, this external load will be replaced with the bridle force measured by the dynamometer when we replace the entire downhole suck rod pump system with the Maxwell viscoelastic model. Again, we can imagine that in relaxation test, we can simply add a dead weight W_o in addition to the

weight of the mass m. Using the same kinematic and dynamic procedures, assuming the force in the dashpot and stiffness series as F_o, consider each section in series and the consequent continuity of axial forces, we have

$$F - mu = k\ddot{u} + F_o,$$
$$\dot{u} = \frac{\dot{F}_o}{k_o} + \frac{F_o}{c_o}.$$

Using the kinematic relationship $u(t)=u_1(t)+u_2(t)$, hence $\dot{u}(t) = \dot{u}_1(t) + \dot{u}_2(t)$, we obtain the following third-order governing equation for u(t),

$$\frac{m}{k_o}\dddot{u}_2 + \frac{m}{c_o}\ddot{u}_2 + \frac{k+k_o}{k_o}\dot{u}_2 + \frac{k}{c_o}u = \frac{\dot{F}}{k_o} + \frac{F}{c_o}$$

Let's look at two special cases. First of all, with no dashpot, namely, $c_o=0$. In this case, we have $F_o=0$, hence the governing dynamic equation yields the familiar spring-mass vibration system

$$m\ddot{u} + c_o\dot{u} + ku = F(t)$$

The second special case corresponds to the infinitely stiff spring k_o, namely, $k_o \to \infty$, consequently, $k_o \to \infty$ and $u(t)=u_1(t)$. Finally, we recover the familiar spring-mass-dashpot vibration system

$$m\ddot{u} + c_o\dot{u} + ku = F(t)$$

Again, to facilitate the solution, we can rewrite the third-order viscoelastic vibration system with a dynamical system format,

y=Ay+f

with the state variable $\mathbf{y} =< u_2, \dot{u}_2, \ddot{u}_2 >$, and

$$\mathbf{A}=\begin{bmatrix} 0 & 1 & 0 \\ 0 & 0 & 1 \\ -\frac{kk_o}{mc_o} & -\frac{k+k_o}{m} & -\frac{k_o}{c_o} \end{bmatrix} \text{ and } \mathbf{f}=\begin{bmatrix} 0 \\ 0 \\ \frac{\dot{F}}{m} + \frac{k_oF}{mc_o} \end{bmatrix}$$

In the following two examples, we employ k=4 N/m, m=1 kg, c_o=0.2 Ns/m, k_o=4 N/m, and W_o=10 N. Both viscoelastic vibration models will start from the zero position with zero velocity and zero acceleration. The external force F(t) is a dead weight W_o. Based on the Mathworks Matlab simulation, it is clear that the vibration eventually settles down to an equilibrium position due to the dashpot damping. Of course, in this paper, we will replace the deadweight with the actual bridle force measured with the dynamometer.

As shown in Figs. 4 and 5, even with a very preliminary Kelvin and Maxwell model, we can still recreate the hysteresis loop of load and displacement for the sucker rod pump system. In the simulation, the magnification factor is 85 for both Maxwell and Kelvin model to match the actual large motion of the sucker rod with the viscoelastic model in the simulation. Notice again that the load F(t) used in the viscoelastic model is the exact load measurement recorded in one of the TAM software examples.

An improvement Kelvin viscoelastic vibration system with adjusted parameter m, c_o, and k_o demonstrates a much closer displacement response with the measured force F(t) as shown in Fig. 6. In general, by reducing the parameter m, the peak of the displacement will shift to the left, which corresponds to the increase of the natural frequency and by increasing the parameter c_o, the viscous damping is increased and the starting and the ending points will be closed. Finally, by increasing the stiffness parameter k_o, the end displacement tends to increase.

EXPERIMENTAL SETUP

In the sucker rod experimental setup with horizontal configuration established in McCoy Engineering Hall at Midwestern State University as shown in Fig. 7, we have one solenoid valve with four ports and three positions. The physical model is depicted in Fig. 8. The chamber A near the cap end corresponds to the sucker rod pump unit, the plunger with a length L is the exactly same plunger used in petroleum industries. The chamber B near the rod end represents the oil well section above the sucker rod pump. To ensure the air and liquid tight, we use the same stuff box to support the retracting sucker rod physically attached to the plunger. Moreover, a positive measure system LVDT is installed at the tip of the sucker rod. Transient pressure within both chambers A and B will be measured with a sampling rate of 30 samples per second or 30 Hz using the Echometer pressure measurement system.

The external horizontal forces acting on the plunger are depicted in Fig. 8. Assume the atmospheric pressure p_{atm} and the plunger is moving at this time instant with a velocity V to the left, a positive direction in this case, we have viscous shear force F_v acting on plunger to the right. Furthermore, the pressure in chamber A denoted as p_A exerts on the plunger a horizontal force $F_A = p_A \frac{\pi D_i^2}{4}$ to the left whereas the pressure in chamber B denoted as p_B exerts on the plunger a horizontal force $F_B = p_B \pi \frac{D_i^2 - D_a^2}{4} + p_{atm} \pi \frac{D_a^2}{4}$ to the right.

Since the plunger as illustrated in Fig. 8 at this time instant is moving to the left, the pressure in chamber A must be higher than the pressure in chamber B. The Poiseuille flow due to pressure difference, as the primary contribution of leakage, is to the left, whereas the Couette flow due to the boundary shear motion, as the secondary contribution of leakage, is to the left, in the same direction as the velocity V at this time instant.

As illustrated in Fig. 8, consider the plunger with an outer diameter D_i and the barrel inner diameter D_o. Assume the gap d denoted as $\frac{D_o - D_i}{2}$ is small in comparison with D_o and D_i. In engineering practice, the clearance C is equivalent to 2δ with $\varepsilon = \frac{2\delta}{D_i}$.

For Poiseuille flow, following the discussion in our earlier paper on leakage Ref. 7, we obtain the leading terms of the corresponding flow rate Q_p

$$Q_p = \frac{\pi(p_A - p_B)}{12\mu L} D_i \delta^3$$

where μ is the dynamic viscosity of the hydraulic fluid we use in this setup.

As a consequence, the viscous shear force F_p acting on the plunger surface in the direction from the chamber A to the chamber B can be calculated as

$$F_p = \pi(p_A - p_B) D_i \frac{\delta}{2}$$

For Couette flow, following the discussion in our earlier paper on leakage Ref. 7, we obtain the leading terms of the corresponding flow rate Q_c

$$Q_c = \pi V D_i \frac{\delta}{2}$$

As a consequence, the viscous shear force F_v acting on the plunger surface in the direction from the top to the bottom can be calculated as

$$F_c = \frac{\pi L \mu D_i V}{\delta}$$

Overall, the flow rate Q to the left with a plunger velocity V to the left is calculated as $Q=Q_c+Q_p$, whereas the shear force to the right is calculated as $F_v= F_{c-} F_p$. Notice the proportionality to the velocity V and the sign change for the shear flow. This is due to the Poiseuille flow direction which is from the chamber A to the chamber B. Assume the hydraulic system has the flow rate Q_o and the corresponding power is

$$P_h = Q_o(p_A - p_B)$$

The following two governing equations are the key to analyze the experimental data. First of all, the kinematic relationship with regard to the cap end cavity or control volume. Assume the rod displacement is U(t), the change of the cap end volume is then depicted as

$$\dot{U}\pi\frac{D_o^2}{4} = Q_o - Q$$

with $V = \dot{U}$.

Notice that this relationship only holds for the cap end since the stuff box side or the rod end is not exactly fully sealed. Secondly, we must observe the dynamical balance of the plunger. Assume the total mass of the plunger with the polish rod is M, we have

$$F_s - F_d + F_A - F_B = M\dot{V}$$

A preliminary measure for the vertical orientation of our experimental setup is presented in Fig. 9 and the detailed study of this complicated set of kinematic and dynamic governing equations will be presented in next year's Southwestern Petroleum Short Course.

CONCLUSION

In petroleum industry, it is not desirable to completely eliminate the leakage due to the pressure differential which could be as high as a few thousand *psi* because we must limit the contact as well as the wear and tear of the sucker rod pump plunger and the pump barrel. Furthermore, by reserve a slight gap between the plunger and the pump barrel, the sucker rod pump will also be able to operate in oil field with the pollution of sands. The main purpose of this research paper is to provide a better understanding along with quantifiable relationship with respect to the leakage and many relevant operational conditions such as the pressure differential and viscous shear. Leakage issue is multifaceted and complex. For complicated problems such as this, simple analytical, or computational, or empirical studies alone are not sufficient. This revisit of leakage issue has established some useful information, such as the relative importance of leakage and hysteresis loop due to Poiseuille flow and Couette flow, time scale for the transient effects, and effects of eccentricity. Therefore, a combination of analytical and computational approaches is presented with comparison to existing empirical measurements. This viscoelastic study of the downhole conditions of sucker rod pump system will shed new light on the mechanisms of hysteresis loops of individual pump system and pinpoint the key physics with relevance to the surface displacement and the bridle force which could be measured.

ACKNOWLEDGEMENT

We would like to thank Mr. Jim McCoy and his Echometer Company and Brad Rogers in Dover Artificial Lift, Harbison-Fischer for providing relevant information and financial support for this study.

REFERENCES

1) J.F. Lea (2012b). What's new in artificial lift? *World Oil*, pages 85--94. Part II.

2) J.M. Nouri and J.H. Whitelaw (1994), Flow of Newtonian and non-Newtonian fluids in a concentric annulus with rotation of the inner cylinder. *ASME Journal of Fluids Engineering*, 116(4):821--827.

3) P.M. Bommer and A.L. Podio (2012). The Beam Lift Handbook. *PETEX*.

4) G. Takacs (1993). Modern sucker-rod pumpin, *PennWell Books*.

5) G. Takacs (2015). Sucker-rod pumping handbook - production engineering fundamentals and long-stroke rod pumping. *Elsevier Science*.

6) S. Wang (2008). Fundamentals of Fluid-Solid Interactions-Analytical and Computational Approaches. *Elsevier Science*.

7) S. Wang, L. Rowlan, M. Elsharafi, M.A. Ermila, T. Grejtak, and C.A. Taylor (2019). On leakage issues of sucker rod pumping systems. *ASME Journal of Fluids Engineering*, 141(11):111201--7.

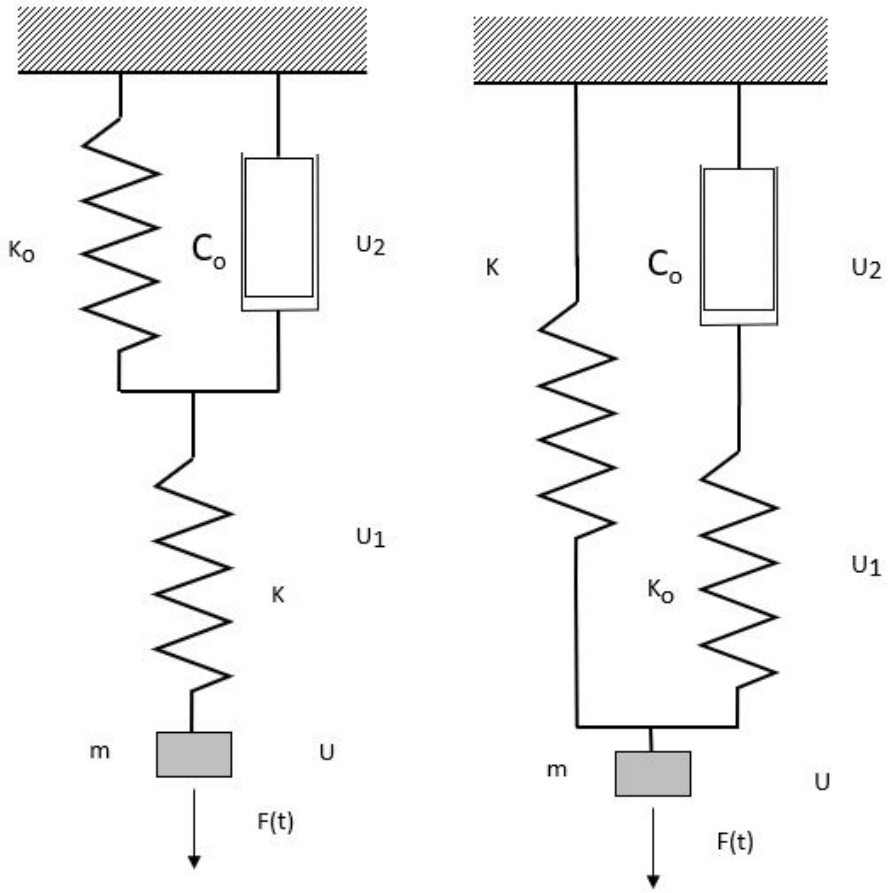

(a) Kelvin Vibration Model (b) Maxwell Vibration Model

Figure 1. Kelvin and Maxwell viscoelastic vibration models.

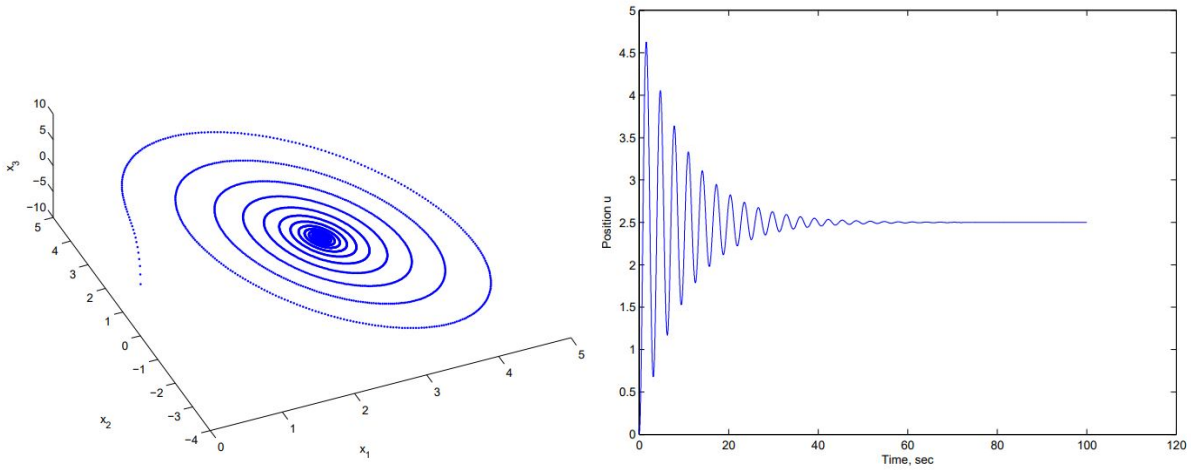

(a) Phase diagram (b) Mass displacement

Figure 2. Kelvin viscoelastic vibration system with a constant force F(t).

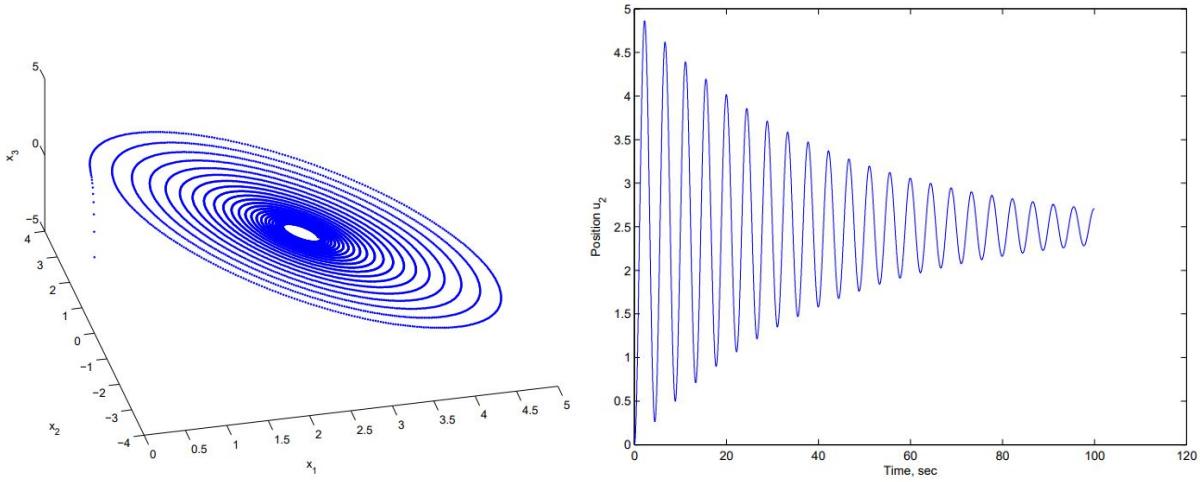

(a) Phase Diagram (b) Mass displacement

Figure 3. Maxwell viscoelastic vibration system with a constant force F(t).

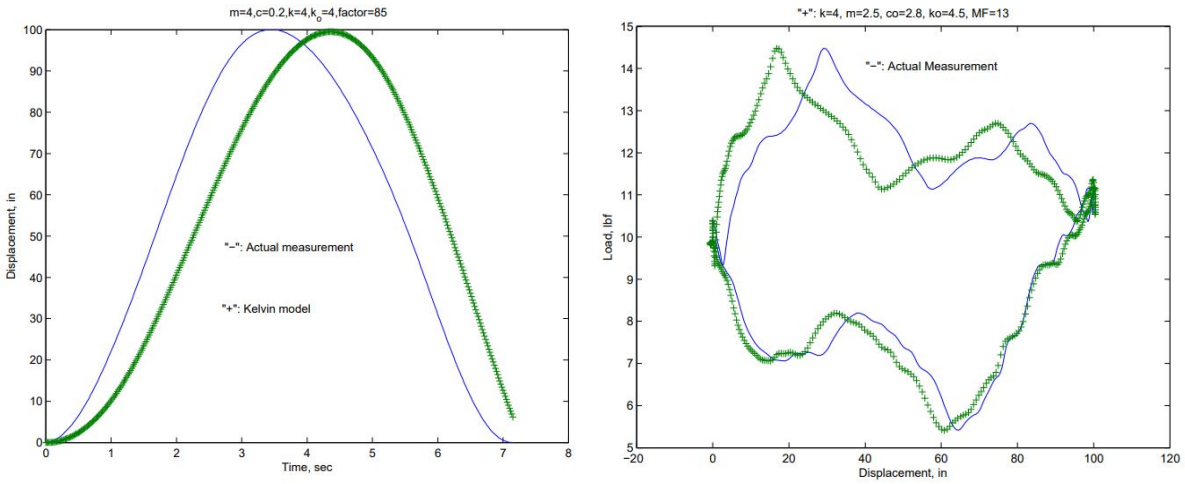

(a) Displacement (b) Force-Displacement hysteresis loop

Figure 4. Kelvin viscoelastic vibration system response and hysteresis loop.

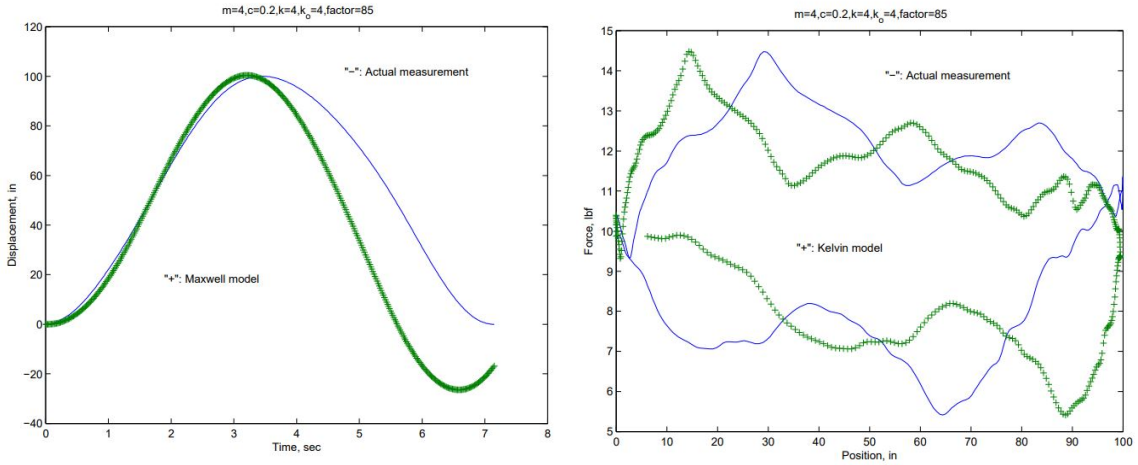

(a) Displacement (b) Force-Displacement hysteresis loop

Figure 5. Maxwell viscoelastic vibration system response and hysteresis loop.

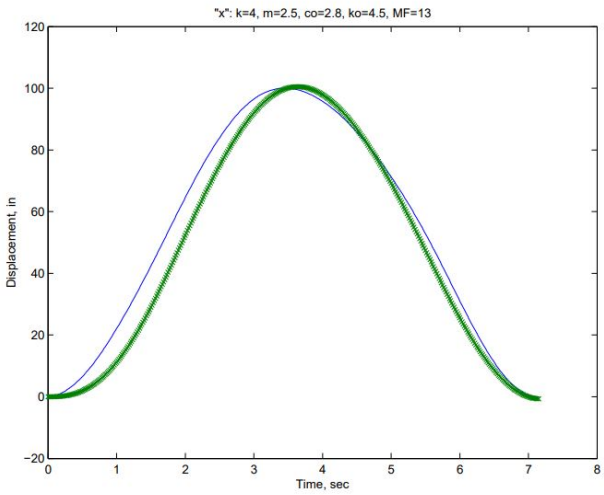

(b) Displacement

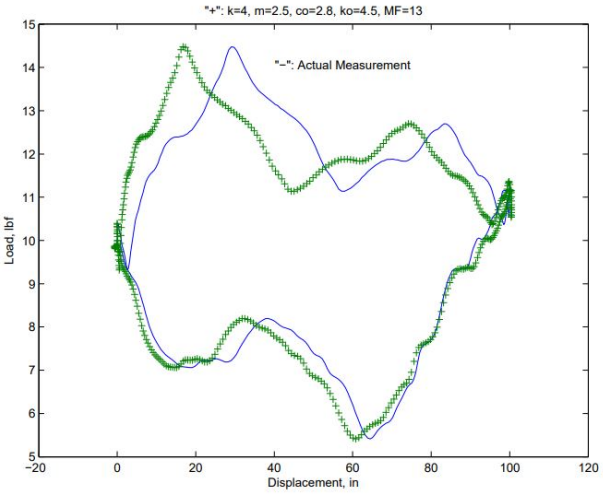

(b) Force-Displacement hysteresis loop

Figure 6. An improved Kelvin viscoelastic vibration system response and hysteresis loop.

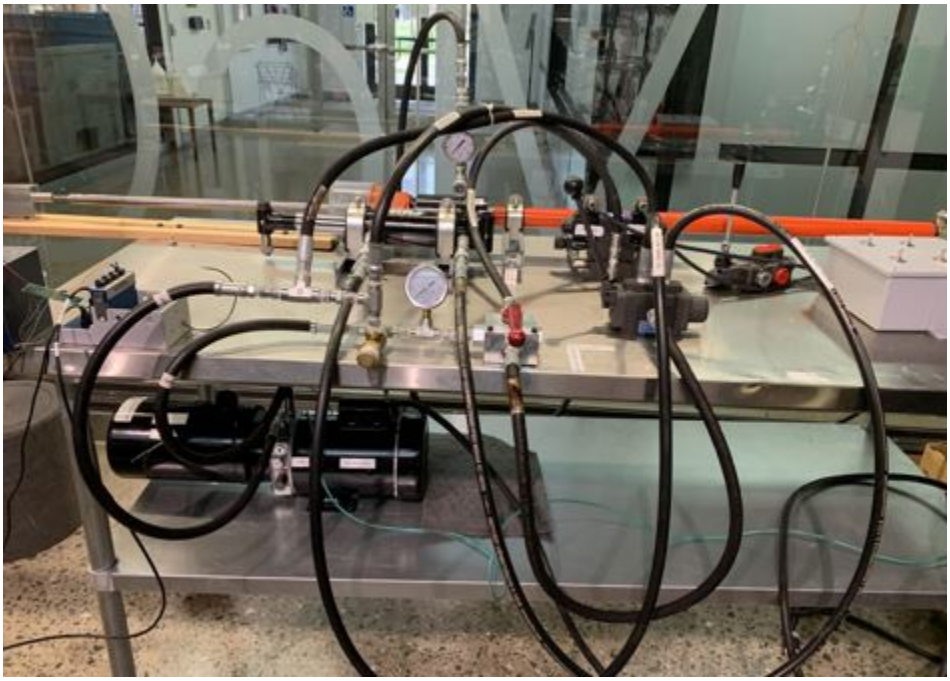

Figure 7. Horizontal sucker rod experimental validation system at MSU Texas.

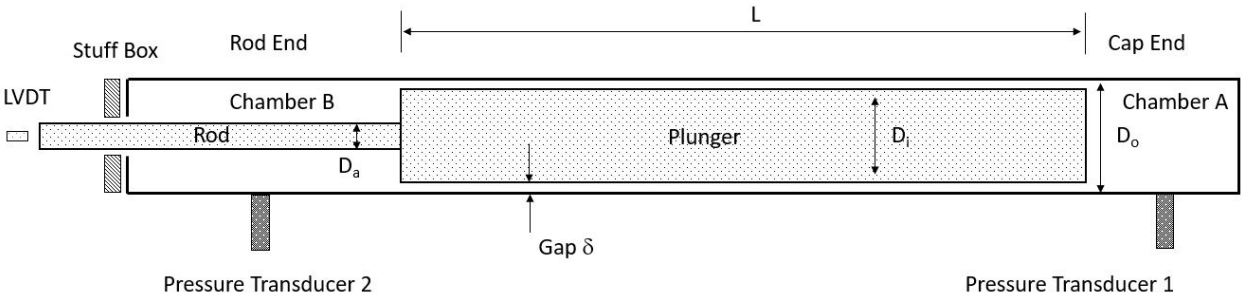

Figure 8. Sucker rod experimental validation system model.

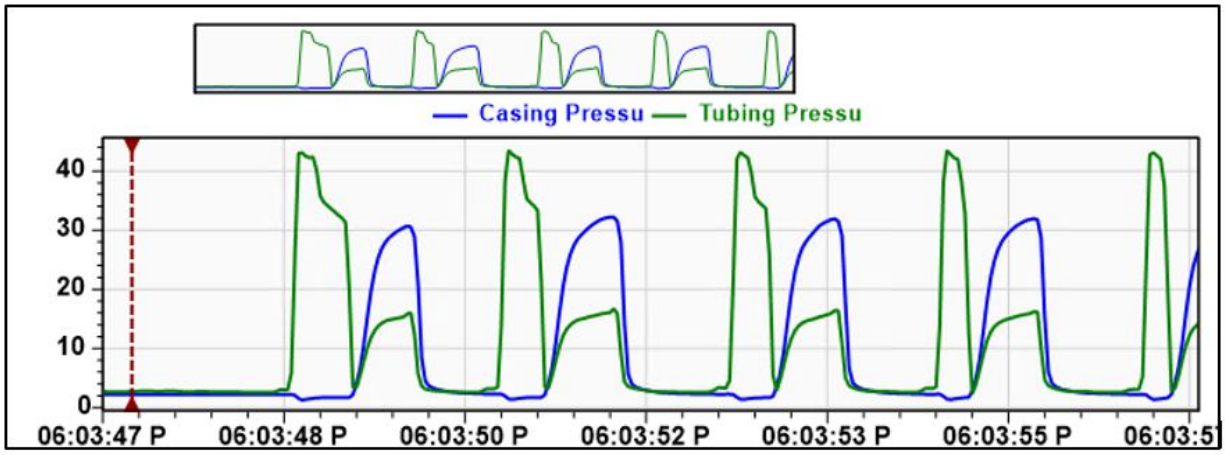

Figure 9. Echometer pressure measurement interfaces for vertical configuration.